Korean J. Chem. Eng., 33(4), 1480-1488 (2016)
DOI: 10.1007/s11814-015-0259-8

pISSN: 0256-1115
eISSN: 1975-7220

Photoisomerization behavior of photochromic amide-based azobenzene dyes exhibiting H-bonding effect: Synthesis and characterization

Gurumurthy Hegde*,†, Yuvaraj Aralapura Rajkumar, Gan Siew Mei**, Syed Mahmood***, Uttam Kumar Mandal***, and Achalkumar Ammathnadu Sudhakar****

*BMS R and D Centre, BMS College of Engineering, Basavanagudi, Bangalore 560019, India
**Faculty of Industrial Sciences and Technology, University Malaysia Pahang, 26300, Gambang, Kuantan, Malaysia
***Department of Pharmaceutical, Technology, Kulliyyah of Pharmacy, International Islamic University, Malaysia (IIUM), Pahang Darul Makmur, Malaysia
****Department of Chemistry, Indian Institute of Technology, Guwahati, 781039, Guwahati - Assam, India
(*Received 1 July 2015 • accepted 26 November 2015*)

Abstract−Amide linkage was introduced into azo compound at para position and its optical storage properties were investigated. Synthesized compounds showed liquid crystalline behavior when electron withdrawing group was inserted in the chemical structure. UV/Vis study showed that the photoisomerization effect in solution occurred at 18-24 sec (*E-Z*) and 5-11 hours (*Z-E*), whereas in solids it occurred at 30 sec (*E-Z*) and 5 hours (*Z-E*). Photoisomerization effect of amide based azodyes in the presence of hydrogen bonding is discussed for the first time. Effect of terminal electronic withdrawing groups on hydrogen bonding is speculated to be the reason behind the surprising behavior. Strong evidence for the structure property relations reported here is useful for applications such as optical storage device in which one can tune the structure according to one's requirement.

Keywords: Azobenzene, Amide, Hydrogen Bond, Optical Properties, Photoisomerization

INTRODUCTION

Azobenzenes are the most commonly used organic molecules in the application of photo-switches, owing to their efficient light absorption capacity, photoisomerization process and relative molecular shape changes between *Z* and *E* isomers [1]. The ease of synthesis and functionalization probably contribute to its extended application. However, only few reports are available on monodispersed azobenzenes for crystal structure related studies and their photoisomerization effect [2]. Azodyes are considerably good materials for constructing optical storage devices that store the data using light [1,3-5]. This phenomenon of information storing becomes simple due to the *trans-cis* (*E/Z)* photoisomerization and the resulting molecular orientation which contains chromophores that occurs mainly due to the light sensitive azobenzene [6,7]. The process of photoisomerization is initiated by UV light of suitable wavelength and subsequent molecular geometry, which can be controlled by light [7-11]. The molecular re-orientation is accompanied by *E/Z* isomerization of chromophoric groups. Azobenzene moiety is a well-known chromophoric group in the study of reversible photoisomerization [12-15]. The reverse process that occurs without aid of any external stimuli is known as "thermal back relaxation" or *Z* to *E* isomerization and is spontaneous [1,3-7]. Recently, we reported synthesis and optical storage properties of the aromatic and aliphatic spacers incorporated into azodye dimers having aliphatic and aromatic spacers, which was responsible in tuning the chemical structures [16].

On the other hand, the amide group plays an important role in the photoisomerization of azodyes [17]. The synthetic process of amides is involved in the direct combination of carboxylic acid and amines [18]. In between the successive molecules of amides, there is weak hydrogen bonding which may be affected dramatically in the presence of other functional groups [19,20]. The bonded pair of electrons, on the atoms having more electronegativity will be attracted by the hydrogen atoms [21]. This kind of bond formation, which is possible either between the two molecules or in a single molecule, is called intramolecular and intermolecular H-bonding, respectively. In H-bonding, the bond strength increases with increase in electronegativity of the electron-rich species present in the molecules [22]. The hetero-atoms which are present in the organic molecules facilitate the H-bonding effect. In other words, H-bonding restricts the molecular movement [23]. Due to this, the molecular interaction with UV light differs with respect to electron-withdrawing groups present in the molecule.

Herein, for the first time we report the effect of electron withdrawing group at para position to the amide linkage of azodye on their photoisomerization properties. The study reveals the H-bonding effect on the amide based azodyes in the absence and in the presence of electron withdrawing groups. These compounds may find application in the study of optical storage devices.

EXPERIMENTAL SECTION

1. Materials and Methods

The analytical grades of ethyl 4-amino benzoate, sodium nitrite,

†To whom correspondence should be addressed.
E-mail: murthyhegde@gmail.com

1-bromohexane, potassium hydroxide, potassium iodide, aniline, 1, 3-dicyclohexylcarbodiimide (DCC), 4-(N, N-dimethylamino) pyridine (DMAP), 4-nitroaniline (Fluka), potassium carbonate were procured from Sigma Aldrich; and phenol, acetone, 4-amino acetophenone and silica gel-60 were from Merck Laboratory. Acetone and dichloromethane were dried over phosphorus pentaoxide and calcium hydride, respectively. These solvents were distilled before its use in the experiment.

FTIR spectra were recorded using a Perkin Elmer (670) FTIR spectrometer. ^{1}H NMR (400 MHz) and ^{13}C NMR (100 MHz) were recorded on the Bruker. Elemental analysis was done by CHN elemental analyzer (Leco & Co.). The photo-switching study was monitored by using UV-Visible spectrophotometer from Ocean Optics (HR2000+). For photo-switching studies in solutions, amide-based photo-switchable azodyes were dissolved in chloroform at fixed concentration of C=1.1×10^{-5} mol L^{-1}. Photoisomerization of these compounds was investigated by illuminating with an Omnicure S2000 UV source equipped with a 365 nm filter and heat filter to avoid unwanted heat. The intensity used for measuring *E/Z* was 5.860 mW/cm^2 using UV meter. The absorption spectra were taken in both solution and solid state for all the four synthesized compounds. The photo-switching behavior of these compounds was studied by UV light of suitable wavelength. Liquid crystalline properties were investigated by using polarized optical microscopy (Olympus BX51) along with linkam hotstage (Linkam). Thermal analysis measurements were done by Mettler Toledo DSC 1 under nitrogen atmosphere from RT to 200 °C at the rate of 5-10 °C/min.

1-1. Ethyl 4-(4-hydroxyphenylazo) Benzoate (B)

Compound A (46.00 mmol, 1 equiv.) was dissolved in 40 ml of methanol and then cooled to 2 °C. To this solution, 8.672 ml of 25% HCl was added dropwise at 2 °C. Then, $NaNO_2$ (44.6 mmol, 1 equiv.) was slowly added dropwise at 2 °C. The reaction mixture was stirred for about 15 min. To this reaction mixture, phenol solution and methanol (44.6 mmol, 1 equiv.) were added slowly at 2 °C. Then pH (8.5-9.0) was adjusted by adding 1 N NaOH solution. The reaction mixture was stirred for about 4 hr. Then 250 ml of methanol and ice was added to the reaction mixture and pH was adjusted to 4. Finally, the reddish yellow product precipitate was filtered through Whatman filter paper and dried at RT. The crude product was recrystallized twice using methanol as a solvent.

A reddish yellow solid: R_f=0.42 (40% CH_2Cl_2-EtOH); yield: 62%; Melting point: 160.2 °C; IR (KBr Pellet) γ_{max} in cm^{-1}: 3321, 1728, 1602, 1484, 1248, 1140, 829; ^{1}H NMR (400 MHz, Acetone-d6): δ 8.17 (d, J=8.2 Hz, 2H, Ar), 7.92 (d, J=7.5 Hz, 2H, Ar), 7.88 (d, J=7.5 Hz, 2H, Ar), 7.01 (d, J=8.2 Hz, 2H, Ar), 5.54 (s, 1H, OH), 4.42 (q, J=7.2 Hz, 2H, CH_2CH_3), 1.44 (t, 3H, CH_2CH_3); MS (FAB+): m/z for $C_{15}H_{14}N_2O_3$, Calculated: 270.28. Found: 270.08.

1-2. Ethyl 4-[4-(4-hexyloxy) Phenylazo] Benzoate (C)

Compound B (18.5 mmol, 1 equiv.) and 1-bromohexane (37.1 mmol, 2 equiv.) were dissolved in 300 ml of dry acetone. To this, potassium carbonate (18.5 mmol, 1 equiv.) was added portion-wise followed by catalytic amount of potassium iodide (50 mg). Then the reaction mixture was refluxed for about 24 hr under nitrogen atmosphere. The running reaction was monitored using TLC. After completion of the reaction, solvent was removed and the obtained product was taken for the next step.

1-3. 4-[4-(4-hexyloxy)phenylazo] Benzoic Acid (D)

Compound C was dried and dissolved in 100 ml of methanol. The reaction mixture was cooled to 5 °C and then potassium hydroxide (62.2 mmol, 3 equiv.) in water (20 ml) was added dropwise. The reaction mixture was then refluxed for about 4 hr. The reaction was monitored by using TLC method. The reaction mixture was washed with n-hexane (25 ml) two times to remove the nonpolar impurities. Then pH was adjusted to 6 by adding dilute hydrochloric acid. The compound was then extracted in ethyl-acetate, which was followed by washing with brine solution. The ethyl acetate layer was dried over anhydrous sodium sulphate. Then filtered to remove the sodium sulfate and then the clear filtrate was collected. The ethyl acetate solvent was removed by rotor vapor to collect the solid product and recrystallized it from ethanol : chloroform (2 : 1).

A dark yellow solid; yield: 46%; IR (KBr Pellet) γ_{max} in cm^{-1}: 2849, 2918, 3004, 1711, 2918, 1220, 1588, 1493, 1248, 1130, 1092, 835; ^{1}H NMR (400 MHz, DMSO-d6): δ 10.46(s, 1H, COOH), 7.94 (d, J=8.05 Hz, 2H, Ar), -7.89 (d, J=8.10 Hz, 2H, Ar), 7.52 (d, J=8.01 Hz, 2H, Ar), 6.61 (d, J=7.98 Hz, 2H, Ar), 3.91 (t, J=12.01 Hz, 2H, ether), 2.13-0.92 (m, 11H, aliphatic); ^{13}C NMR (100 MHz, DMSO-d6): δ 166 (COOH), 162, 154, 146, 132, 130, 125, 123, 122, 119, 114, 68 (OCH2), 30, 28, 25, 22, 13; MS (FAB+): m/z for $C_{19}H_{22}N_2O_3$, Calculated: 326.39. Found: 326.09.

1-4. 4-[(4-hexyloxyphenyl)diazenyl]-*N*-phenylbenzamide (E)

Compound D (15.3 mmol, 1 equiv.) was dissolved in 50 ml of dry dichloromethane. To this DMAP (1.40 mmol, 0.1 equiv.) was added and the mixture was stirred for about 30 min. A solution of aniline (15.3 mmol, 1equiv.) in dry dichloromethane (10 ml) and DCC (23.0 mmol, 1.5 equiv.) in 10 ml of dry dichloromethane was added slowly. The mixture was stirred for about 24 hr. This reaction was monitored by using TLC. After completion of the reaction, the precipitate formed was removed by filtration and the filtrate was quenched in 1.5 N hydrochloric acid. The compound was extracted with chloroform. The chloroform layer was washed with 1 N sodium hydrogen carbonate, which was followed by a brine wash. Then chloroform was dried over anhydrous sodium sulfate for 1 hr. Finally, the solid crude product was collected by evaporating chloroform. Crude product was purified by column chromatography using chloroform : methanol (20 : 1) as eluent. The product was recrystallized from methanol : chloroform (2 : 1) to get the target compound E_1.

A similar procedure was followed to synthesize the compounds E_2, E_3 and E_4.

E_1: A pale yellow solid; yield: 60%; melting point is 184.5 °C; IR (KBr Pellet) γ_{max} in cm^{-1}: 3325, 3004, 2930, 2852, 1094, 1640, 1500, 1538, 1449, 1248, 1130, 1092, 835. ^{1}H NMR (400 MHz, DMSO-d6): δ 7.95 (d, 1H, CONH), 7.94-7.89 (m, 9H, Ar), 7.52 (d, J= 8.01 Hz, 2H, Ar), 6.61 (d, J=7.98 Hz, 2H, Ar), 3.91 (t, J=12.01 Hz, 2H, ether), 2.13-0.92 (m, 11H, aliphatic); ^{13}C NMR (100 MHz, DMSO-d6): δ 162, 154, 146, 132, 130, 125, 123, 122, 119, 114, 68 (OCH_2), 30, 28, 25, 22, 13; MS (FAB+): m/z for $C_{25}H_{27}N_3O_2$, Calculated: 401.50. Found: 401.18; Elemental analysis: Calculated (found) %: C 74.79 (74.86), H 6.78 (6.69), N 10.47 (10.38) and O 7.97 (7.86).

E_2: A pale yellow solid; yield: 60%; melting point is 183.5 °C; IR

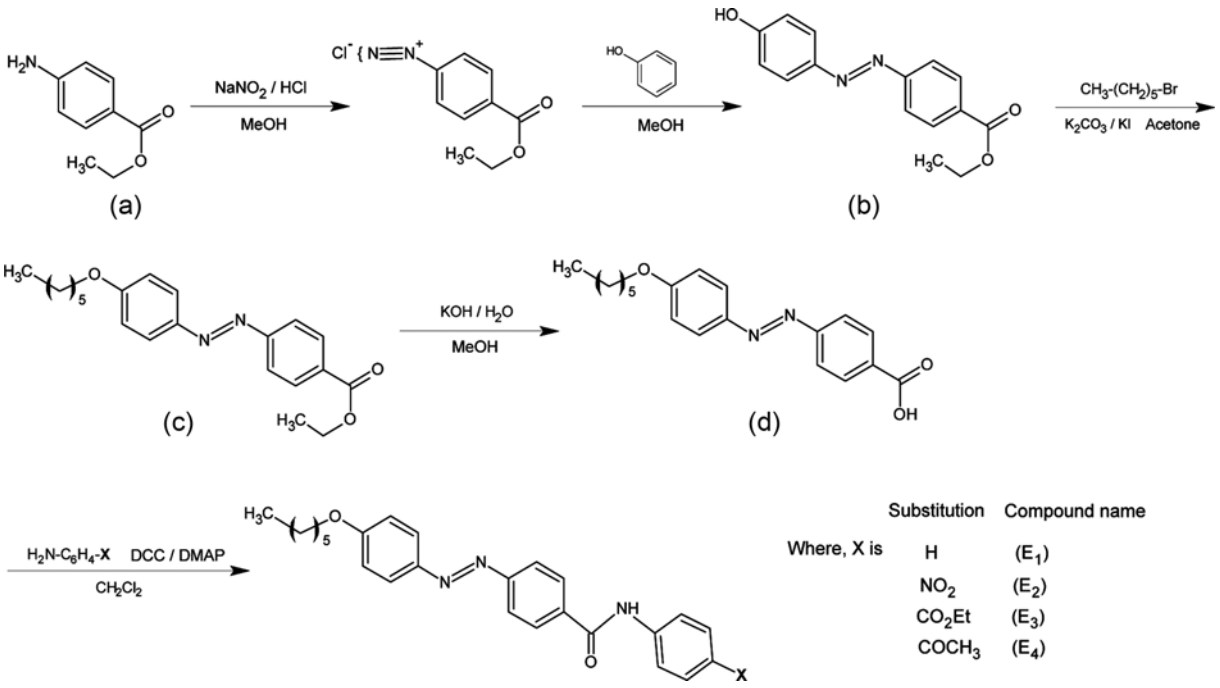

Fig. 1. Scheme of the synthesized compounds reported in this article.

(KBr Pellet) γ_{max} in cm^{-1}: 1520, 1310, 2930, 2851, 3004, 1106, 1640, 3328, 1500, 1538, 1449, 1248, 1130, 1092, 835; ^{1}H NMR (400 MHz, DMSO-d6): δ 8.11 (d, J=8.02 Hz, 2H, Ar), 7.98 (d, J=8.00 Hz, 1H, CONH), 7.93-7.79 (m, 6H, Ar), 7.26 (d, J=8.01 Hz, 2H, Ar), 6.81 (d, J=8.02 Hz, 2H, Ar), 4.40 (t, J=12.00 Hz, 2H, ether), 0.85-2.01 (m, 11H, aliphatic); ^{13}C NMR (100 MHz, DMSO-d6): δ 161.19, 145.81, 130.29, 126.83, 126.74, 124.33, 124.06, 123.41, 121.41, 121.94, 121.57, 121.46, 113.84, 113.76, 68 (OCH_2), 30, 28, 25, 22, 13; MS (FAB+): m/z for $C_{25}H_{26}N_4O_4$, Calculated: 446.50. Found: 446.16; Elemental analysis: Calculated (found) %: C 67.25 (67.34), H 5.87 (5.81), N 12.55 (12.16) and O 14.33 (14.19).

E_3: A pale yellow solid; yield: 60%; melting point is 212.3 °C; IR (KBr Pellet) γ_{max} in cm^{-1}: 1732, 1099, 2930, 2851, 3002, 1106, 1640, 3328, 1520, 1538, 1448, 1248, 1130, 1092, 835; ^{1}H NMR (400 MHz, DMSO-d6): δ 8.29 (d, J=8.03 Hz, 2H, Ar), 7.99 (d, J=8.01 Hz, 1H, CONH), 7.79-7.94 (m, 4H, Ar), 7.64 (d, J=8.01 Hz, 2H, Ar), 7.37 (d, J=8.04 Hz, 2H, Ar), 6.81 (d, J=8.02 Hz, 2H, Ar), 3.41 (m, 2H, ester), 3.98 (t, J=12.01 Hz, 8.00 Hz, 2H, ether), 0.85-2.00 (m, 14H, aliphatic); ^{13}C NMR (100 MHz, DMSO-d6): δ 163, 161, 130, 126.74, 126.62, 124.33, 124.06, 123, 122.03, 121.66, 121.58, 121.49, 113, 113, 68 (OCH_2), 30, 28, 25, 22, 13; MS (FAB+): m/z for $C_{25}H_{26}N_4O_4$, Calculated: 473.56. Found: 473.40; Elemental analysis: Calculated (found) %: C 7 1.01 (71.22), H 6.60 (6.48), N 8.87 (8.77), O 13.51 (13.39).

E_4: A pale yellow solid; yield: 60%; melting point is 185.5 °C; IR (KBr Pellet) γ_{max} in cm^{-1}: 1700, 2852, 2929, 3004, 1092, 1640, 3326, 1578, 1609, 1449, 1248, 1130, 1092, 835; ^{1}H NMR (400 MHz, DMSO-d6): δ 8.29 (d, J=8.00 Hz, 2H, Ar), 7.99 (d, J=8.00 Hz, 1H, CONH), 7.80-7.93 (m, 4H, Ar), 7.64 (d, J=8.02 Hz, 2H, Ar), 7.38 (d, J=8.04 Hz, 2H, Ar), 6.95 (d, J=8.01 Hz, 2H, Ar), 4.00 (t, J=8.00 Hz, 2H, ether), 0.85-2.00 (m, 11H, aliphatic), 3.41 (s, 3H, keto); ^{13}C NMR (100 MHz, DMSO-d6): δ 163, 161, 130, 126.74, 126.62, 124.33, 124.06, 123, 122.03, 121.66, 121.58, 121.49, 113, 113, 68 (OCH_2), 30, 28, 25, 22, 13; MS (FAB+): m/z for $C_{27}H_{29}N_3O_3$, Calculated: 443.54. Found: 443.18; Elemental analysis: Calculated (found) %: C 73.11 (73.23), H 6.59 (6.46), N 9.47 (9.33) and O 10.82 (10.73).

RESULTS AND DISCUSSION

1. Synthesis and Characterization

Synthetic route of 4-[(4-hexyloxyphenyl) diazenyl]-N-phenyl-benzamide (E_1-E_4) with/without electron withdrawing groups at the para position to the amide derived from the 4-[4-(4-hexyloxy) phenylazo] benzoic acid (D) is depicted in Fig. 1. 4-ethyl amino-benzoate was diazotized to yield Ethyl 4-(4-hydroxyphenylazo) benzoate (B). Compound (B) then reacted with 1-bromohexane to give its hexyloxy derivative (C), which on hydrolysis yields acid derivatives (D). Then the amide linkage was introduced into the compound (D) by DCC coupled with anilines having electron withdrawing groups to give the final compounds E_1-E_4.

The structures of the intermediates and desired products were confirmed by recording different spectroscopy techniques such as FTIR, ^{1}H NMR, ^{13}C NMR and CHN elemental analysis. The FTIR spectra of E_1-E_4 exhibited characteristic absorption bands at 1,640 cm^{-1} corresponding to carbonyl group of amide and along with this E_3 and E_4 exhibited a band around 1,732-1,700 cm^{-1} corresponding to carbonyl of ester and ketone, respectively. A band which appeared at 1,449-1,448 cm^{-1} can be assigned to N=N group. With this, all other absorption bands are well observed in the FTIR spectrum for E_1-E_4. A doublet observed in the region 7.99-7.95 ppm is ascribed to amide proton in all the E_1-E_4 [24]. Aromatic protons of E_1-E_4 resonated as multiplets and doublets in the region 8.29-6.61 ppm. Apart from this, all other alkyl, ester and ether protons are

Table 1. DSC thermograms of the compounds E_1-E_4 reported here

Sample code	Electron with drawing groups	DSC (°C)				
		Cr	Heating cooling	N	Heating cooling	Iso
E_1	H (No substituent groups)	*		-	197.67 (3.78) 179.00 (6.17)	*
E_2	NO_2	*	167.61 (5.19) 133.01 (12.29)	*	179.58 (8.59) 160.06 (5.16)	*
E_3	CO_2Et	*	167.78 (7.38) 137.36 (10.20)	*	182.75 (5.43) 155.89 (4.24)	*
E_4	$COCH_3$	*	168.30 (4.82) 147.73 (6.44)	*	185.52 (6.65) 160.25 (5.89)	*

Note: Cr=crystalline phase; N=Nematic phase; Iso=Isotropic phase. Values in bracket corresponds to peak width of the phases. (*=Phase exists; -=phase does not exist)

well observed in the NMR spectrum. The ^{13}C NMR results give the functional group of the carbon as corroborated from the values. Thus, ^{1}H and ^{13}C NMR results are in accordance with the elemental analysis values. Hence, the FTIR, NMR and elemental analysis with mass spectral studies confirms the structures of the compounds E_1-E_4. The thermal behavior of all the compounds was studied using linkam hotstage along with polarized optical microscopy (POM) to check the liquid crystalline behavior of the compounds. Generally, POM is used for textural observation of E_1-E_4 to identify the mesophases. Differential scanning calorimetry was used under nitrogen atmosphere to check the phase transition temperatures of the obtained products.

2. Mesomorphic Properties

The polarizing optical microscopy (POM) texture of the compound E_3 is as shown in Fig. S1. Since all compounds except E_1 exhibit nematic phase, we showed only a representative plot for the same. On cooling from the isotropic state, the nematic (N) phase appears for a short period of time followed by the crystalline phase. So it is usually difficult to capture the nematic phase since its range is too small. Same phenomena are true for all other compounds except compound E_1, which shows only crystal to liquid transition. It means that addition of electron withdrawing groups will help to induce liquid crystallinity in the system. The compounds E_2-E_4 exhibited mesophase both on heating and cooling with enantiotropy. The transition temperatures and associated peak width values obtained from the DSC studies for the compounds E_1-E_4 are summarized in Table 1. DSC thermograms were measured at the rate of 10 °C/min for second heating and cooling. The melting temperature (Tm) of the series is observed in the range of 140-182 °C and the clearing temperature was (Tc) 130-160 °C. The DSC analysis revealed that Tm and Tc of compounds were highly dependent on electron withdrawing nature. It is also evident through DSC thermograms that inclusion of electron withdrawing groups helps to lower the isotropic temperature and phase transition temperatures in comparison with compounds having no electron withdrawing groups. Fig. 2 indicates the DSC thermogram of the representative compound E_3. From Fig. 3, it is evident that the compound E_3 has larger temperature range stability for N phase in

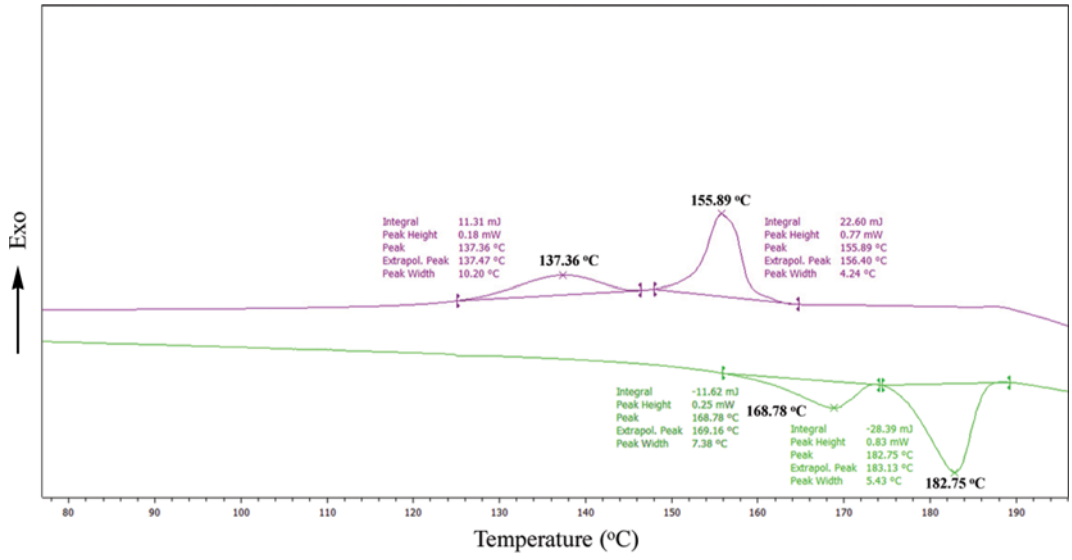

Fig. 2. Representative DSC thermograms of compound E_3.

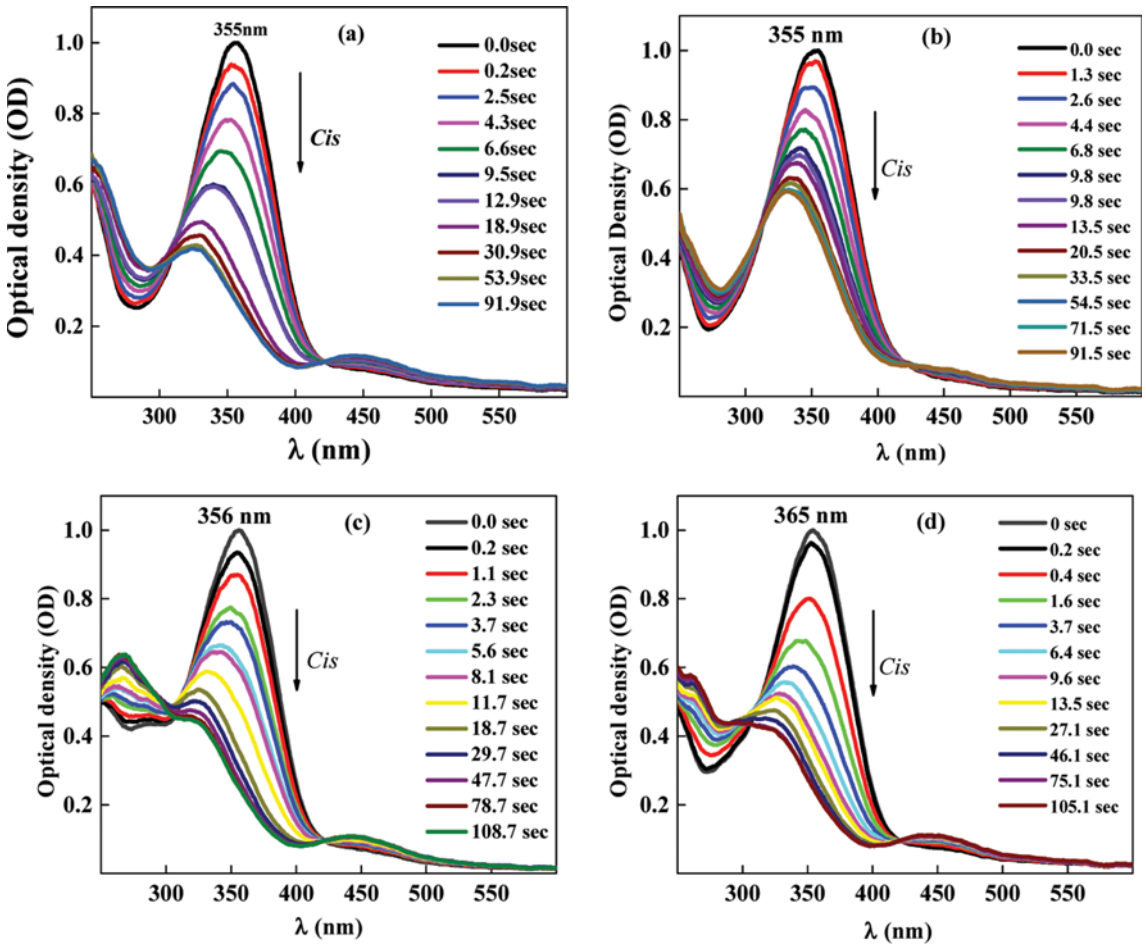

Fig. 3. *E* to *Z* conversion of E_1 (a), E_2 (b), E_3 (c) and E_4 (d) is done by shining UV light at 365 nm.

comparison with other compounds. All DSC measurements are given in Fig. S2-S4.

3. Photoswitching Properties

All the four synthesized azodyes (E_1-E_4) exhibited similar absorption spectra, which is due to the similarity in their molecular structures (see supplementary section Fig. S5). Photoswitching studies were initially performed with solutions and then on solid cells with guest-host system. Here amide based azodye acts like the guest and commercial liquid crystal MLC 6873-100 acts like the host. This gives an insight into the behavior of materials with respect to UV light, and also these results are indispensable for creating optical storage devices [25].

The photoswitching properties of E_1-E_4 were investigated on solutions with illumination of ~365 nm UV light having the intensity of 5.860 mW/cm^2. Fig. 3(a)-(d) depicts the *E/Z* absorption spectra of E_1, E_2, E_3 and E_4 before and after UV illumination, respectively.

The strong absorbance in the UV region at ~355 nm corresponds to π-π* transition of the *E* isomer (*trans* isomer), and a very weak absorbance in the visible region at ~450 nm represents n-π* transition of the *Z* isomer (*cis* isomer) [16,25-27]. The decrease in absorption maxima is due to *E/Z* photoisomerization, which suggests that the *E* isomer is being transformed into the *Z* isomer. The photosaturation values of all the four compounds in solutions are 18, 20, 22 and 24 s, respectively.

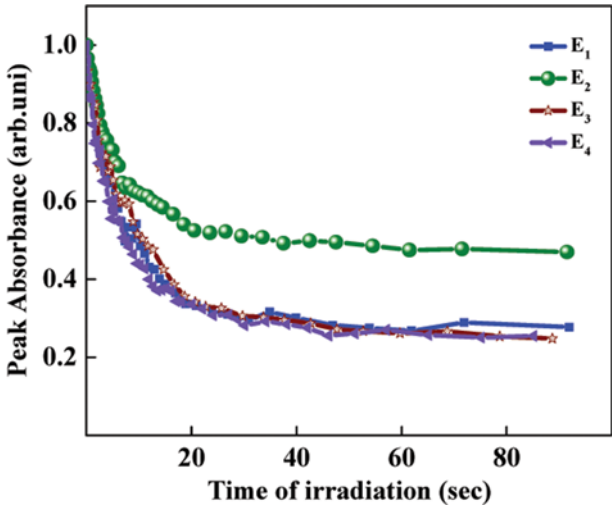

Fig. 4. The absorbance of E_1-E_4 with respect to the function of irradiation time for *E/Z* isomerization. Data abstracted from Fig. 3.

Fig. 4 shows the *E-Z* absorption of compounds E_1, E_2, E_3 and E_4 as a function of exposure time. The peak absorbance were extracted from Fig. 3(a)-(d) by considering the peak wavelength as a function of exposure time. The absorption values of these peak wavelengths

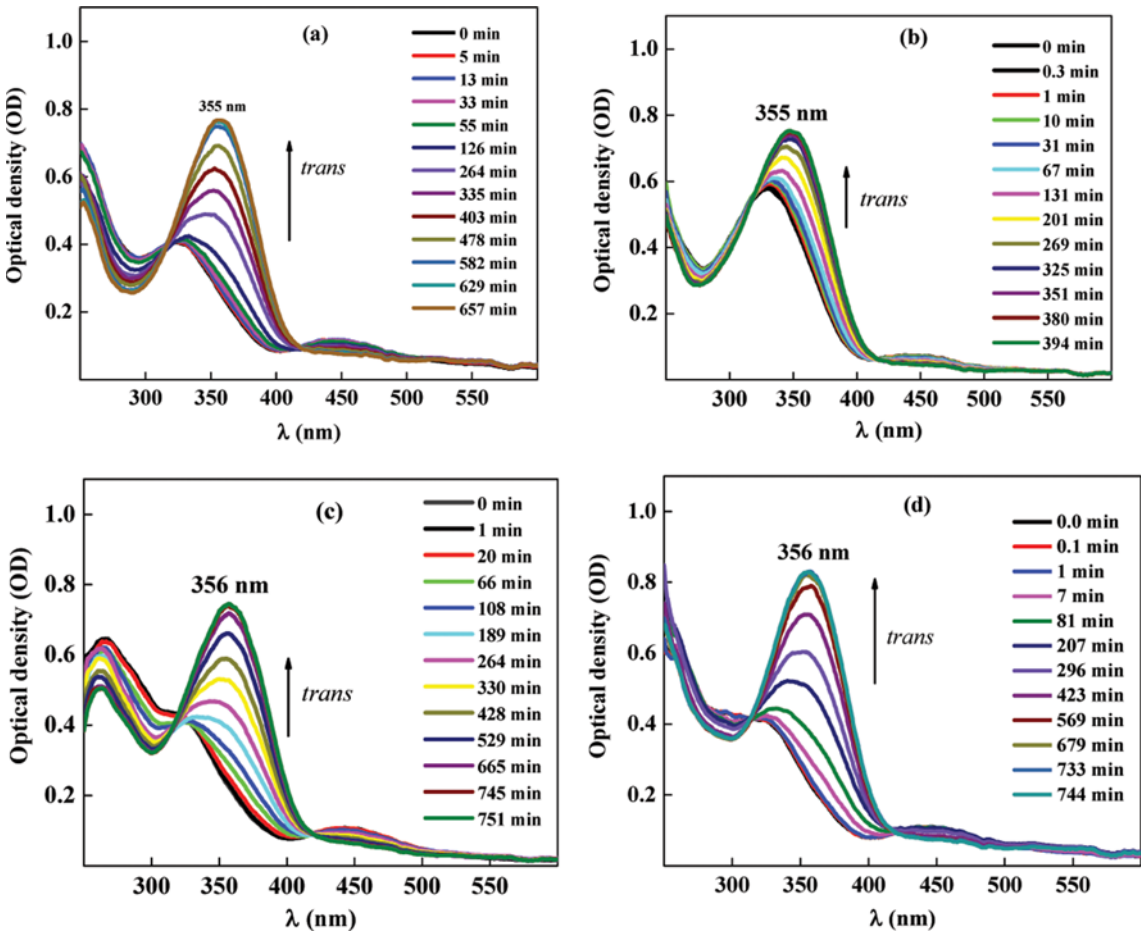

Fig. 5. Thermal back relaxation of *Z/E* transformation of the compounds E_1 (a), E_2 (b), E_3 (c) and E_4 (d). Samples were shined until photosaturation state and data is recorded at RT in dark condition.

with different exposure times were recorded. The curve shows that the time involved in photoisomerization is within 20-24 s.

The *Z* to *E* isomerization can be brought by two methods: one by keeping the solution in the dark, which is called thermal back relaxation, and second by shining white light of higher wavelength. In the present study the thermal back relaxation of compounds was determined by illuminating continuously for ~24 s (photostationary state) and then kept in the dark. Then the spectral data were recorded at subsequent intervals of time. The back relaxation of compounds E_1, E_2, E_3 and E_4 is 9.21, 5.73, 10.18 and 10.58 hr, respectively (Fig. 5(a)-(d)).

The time dependent *Z*–*E* absorption spectra of compounds are as shown in the Fig. 6, which is extracted from Fig. 5(a)-(d). The absorption peak at ~355 nm was fixed and plotted as a function of thermal back relaxation time.

All the four compounds show different interval of thermal back relaxation. A possible reason for the difference in thermal back relaxation could be that the properties of terminal functional groups and the change that occurs are confined to in-plane rotation of the molecules. Due to the effect of functional groups, the optical activity of the compounds may change to a significant extent. It is evident that a mesomeric effect or a hyper conjugation effect plays a significant role in changing the optical properties, which is explained later.

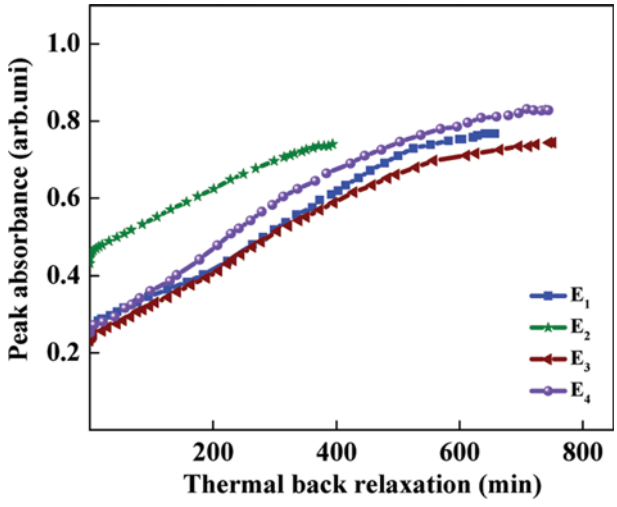

Fig. 6. The absorbance of E_1-E_4 with respect to the function of recovery time for *Z/E* isomerization. Data abstracted from Fig. 5.

To check the intensity dependence, compound E_4 was studied typically as a function of UV intensity. E_4 was shined for 24 s (photo saturation state) with UV light at different intensities (Table S1). As

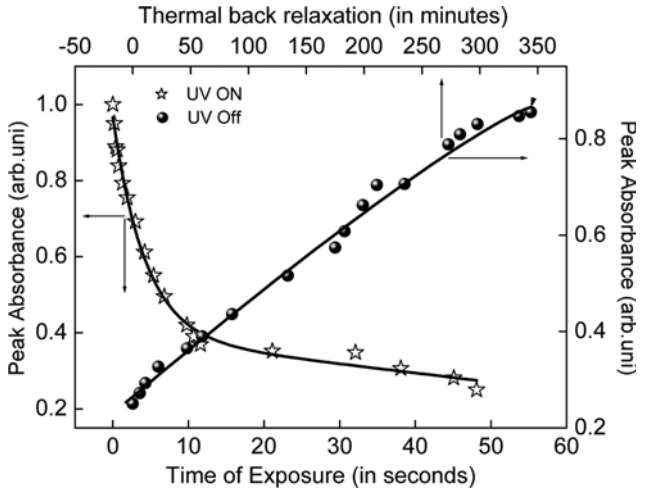

Fig. 7. *E/Z* and *Z/E* isomerization of E_4 with the solid cell. Intensity used is 5.860 mW/cm^2. Guest-host effect is employed where E_4 act like guest and MLC 6873-100 is act like host.

the intensity increased, thermal back relaxation decreased, which is evidently due to the molecular movement.

Spectral investigations on solid cell involved constructing ITO coated, polyimide rubbed glass plates. The mixture was prepared by physically mixing 5% of E_4 in 95% of commercial liquid crystal, MLC6873-100. The mixture was filled by using capillary action into the previously constructed cells. Fig. 7 shows the *E/Z* photoisomerization of solid cell. The intensity of 5.860 mW/cm^2 was used for achieving photosaturation. The photosaturation occurred around ~30 s and the complete thermal back relaxation was observed at ~300 min.

To see the potential ability of the reported materials, we fabricated the device, as shown in Fig. 8, by dissolving 5% of E_4 in 95% of commercially available liquid crystal MLC 6873-100. The material transforms from the ordered state to the disordered state with the illumination of light, giving high contrast between bright and dark states. Dark part of the image corresponds to the shined area,

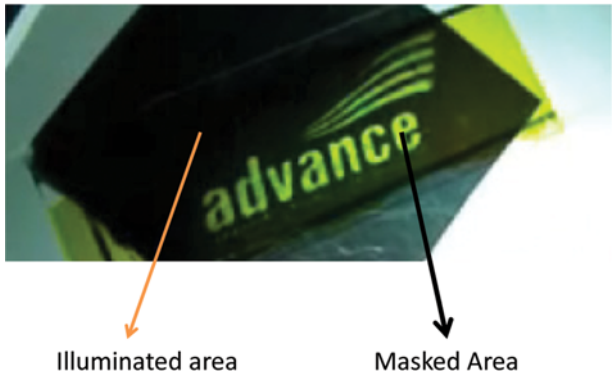

Fig. 8. Demonstration of the optical pattern storage capability of the device based on the principle described in this article. The sample was kept at room temperature and illuminated with UV radiation through a photomask. The dark regions indicate where the molecules are exposed by the passing of the UV and the bright regions are where the radiation is masked.

which transforms from nematic to isotropic state, whereas the latter corresponds to the masked area in which materials remain in nematic state only.

4. The Extent of Photoisomerization or Conversion Efficiency (CE)

The extent of photoisomerization or the conversion efficiency (CE) of the *E/Z* photoisomerization is calculated from the equation below [28].

$$CE = \frac{A(t_0) - A(t_\infty)}{A(t_0)} \times 100$$

where, A (t_0) and A (t_∞) are before and after absorbance, respectively.

The conversion efficiency is very important in describing the photoswitching property of azodyes. The conversion efficiency of E_1-E_4 is as presented in Table S2. CE is comparatively less in azodye materials. The extent of isomerization decreases in presence of amide linkage, in comparison with compounds which do not contain the amide moiety. This decrease in isomerization is due to the presence of intermolecular hydrogen bonding. To justify the lowering extent of isomerization due to hydrogen bonding effect in the amide linkage, the intermediate compound D was studied. Later, the CE of compound D was compared with compound E_1 to clarify and confirm the result. The absorption spectra of compounds D and E_1, before and after shining UV light, are depicted in Fig. S6.

In case of compound D, the extent of isomerization is 85%, whereas 72% of CE was observed in compound E_1. This indicates that the CE decreases with the amide substitution, due to the interaction of electrons and hydrogen atoms in the amide moiety and can be deduced in terms of hydrogen bonding effect.

5. Hydrogen Bonding and Electronic Properties

Difference in photosaturation and thermal back relaxation for E_2, E_3 and E_4 along with their electronic properties is as shown in Table 2. The possible reason for this may be the mesomeric effect as well as hyper-conjugation effect. Inter-molecular hydrogen bonding exists between the molecules (Fig. S7), and the hydrogen bonding restricts the free movement of the molecules to a significant extent. Also, the different functional groups vary the effect of intermolecular hydrogen bonding to a greater extent.

In case of E_1, there is no functional group at the para position with respect to amide moiety. The time required for photosaturation is 18 s and thermal back relaxation is 9.21 hr. So, there is no electronic effect and hence the hydrogen bonding will remain stable.

A strong electron withdrawing group -NO_2 induces positive mesomeric effect for the compound E_2 (refer to Table 1). Once UV is shined on the system, the molecules gain energy. Also, there is a strong positive mesomeric effect exerted by the electron withdrawing -NO_2 group. This leads to the hyper-conjugation effect at N-H moiety of amide as shown in Fig. 9. As a result, inter-molecular hydrogen bonding breaks and molecular movement will become easy, resulting in a fast thermal back relaxation time.

In case of E_3 (-$COOC_2H_5$) and E_4 (-$COCH_3$), which are not having strong electron withdrawing group like -NO_2 get attached to para position with respect to amide moiety. These functional groups have less electron withdrawing nature due to the inductive effect in comparison with -NO_2. Hence, the mesomeric effect is not considerable. Due to the presence of excess oxygen atoms in the form

Table 2. Description of electronic effect with photoisomerization where electron withdrawing group shows fast and slow thermal back relaxation times based on their nature

Compound name & structure	Electronic properties with respect to the terminal functional groups	Photo-isomerization	
		Photosaturation (s)	Thermal back relaxation (hr)
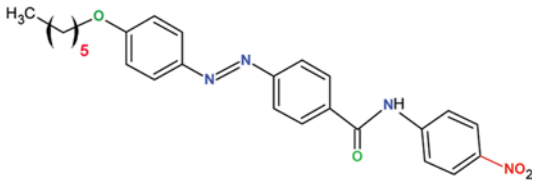 **(E_2)**	-NO_2 causes more "+M effect"	20	5.73
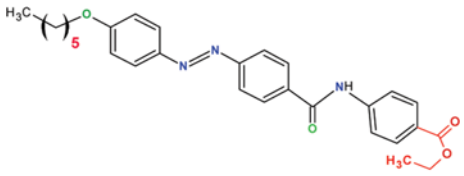 **(E_3)**	-$CO_2C_2H_5$ causes less "+M effect"	22	10.18
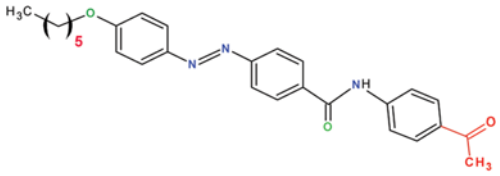 **(E_4)**	-$COCH_3$ causes further less "+M effect"	24	10.58

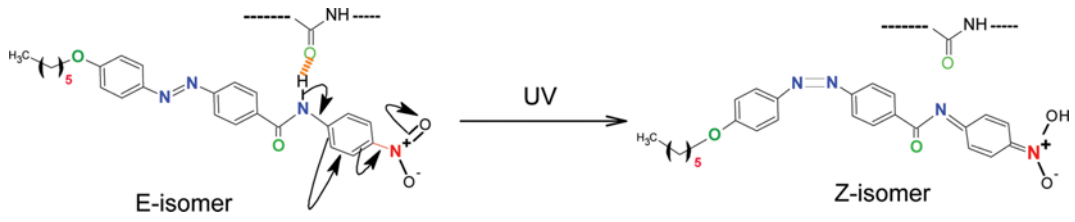

Fig. 9. Hyper conjugation effect in presence of strong electron withdrawing -NO_2 group.

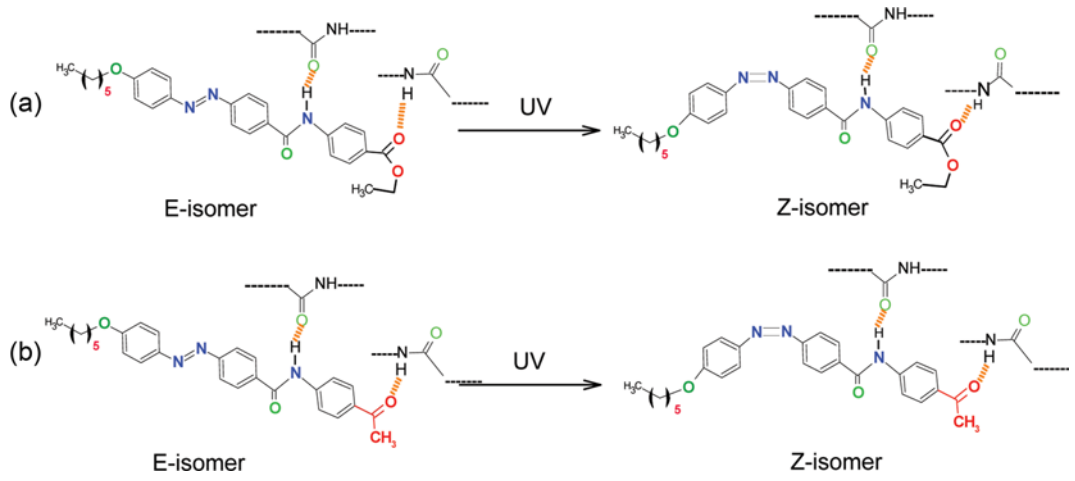

Fig. 10. Stable intermolecular H-bonding in presence of ester (a) and ketone (b).

of ester and ketone, the extent of inter molecular hydrogen bonding will be more as presented in Fig. 10.

Hence, the molecular movement is restricted in these two compounds to a greater extent. As a result, the compounds E_3 and E_4 show very long back relaxation time of about ~10.5 hr. Another reason might be the terminal alkyl chain [19], which helps to restrict the movement.

Thus, a compound with strong electron withdrawing group shows fast back relaxation time, whereas the less strong electron withdrawing group shows slow thermal back relaxation time. Hence, the H-bonding effect is crucial for tuning molecules for optical storage device. This structure property relation plays a dominant role in understanding the phenomena that exist in the molecules and their light behavior.

CONCLUSION

A new series of amide-based azobenzene having different terminal functional groups were synthesized. The effect of electron withdrawing groups is quite interesting, as they contribute to the liquid crystalline nature in the molecules. The photoswitching properties of these materials showed *E-Z* isomerization at 18-24 s and the reverse process occurred at 5-10 hr in solutions, whereas *E-Z* photoisomerization took around 10 s and *Z-E* around 285 min on solids. The presence of amide linkage in azodyes played an important role in photoisomerization. The hydrogen bonding effect is considerable in the optical properties of the compounds and the insertion of electron withdrawing groups makes a dramatic change. Thus, the photoswitching behavior of the materials such as E_1, E_2, E_3 and E_4 could be suitably useful in the field of optical data storage devices and in molecular switches.

ACKNOWLEDGEMENTS

We sincerely acknowledge BMS R and D Centre, BMS College of Engineering for providing the necessary facilities.

Electronic Supplementary Information (ESI) available: [details of any supplementary information available should be included here]. See DOI:10.1039/b000000x/

SUPPORTING INFORMATION

Additional information as noted in the text. This information is available via the Internet at http://www.springer.com/chemistry/journal/11814.

REFERENCES

1. M. L. Rahman, H. Gurumurthy, M. M. Yusoff, M. N. F. A. Malek, H. T. Srinivasa and S. Kumar, *New J. Chem.*, **37**, 2460 (2013).
2. Z. Zhang, H. Xu and Zheng C, *Korean J. Chem. Eng.*, **30**, 2219 (2013).
3. S. M. Gan, Z. F. Pearl, A. R. Yuvaraj, M. R. Lutfor and H. Gurumurthy, *Spect. Acta Part A*, **149**, 875 (2015).
4. A. R. Yuvaraj, T. N. W. Chan, P. G. Yit and H. Gurumurthy, *Spect. Acta Part A*, **135**, 1115 (2014).
5. S. M. Gan, A. R. Yuvaraj, M. R. Lutfor, M. Y. Mashitah and H. Gurumurthy, *RSC Adv.*, **5**(9), 6279 (2015).
6. H. M. D. Bandara and S. C. Burdette, *Chem. Soc. Rev.*, **41**, 1809 (2012).
7. C. G. Iriepa, M. Marazzi, L. M. Frutos and D. Sampedro, *RSC Adv.*, **3**, 6241 (2013).
8. A. A. Beharry and G. A. Woolley, *Chem. Soc. Rev.*, **40**, 4422 (2011).
9. H. Rau, "Photoisomerization of Azobenzenes," In: J. F. Rabek (Ed): *Photochemistry and Photophysic,* CRC Press, Boca Raton, **2**, 119 (1990).
10. Z. Li, Z. Dong, W. Jiabao, C. Biao and L. Haiqing, *Carbohydr. Polym.*, **99**, 748 (2013).
11. J. Lv, W. Wang, J. Xu, T. Ikeda and Y. Yu, *Macromol. Rapid. Commun.*, **35**, 1266 (2014).
12. Z. Yu, S. Hecht and J. Gesel, *Angew. Chem. Int. Ed.*, **52**, 13740 (2013).
13. D. Ishikawa, E. Ito, M. Han and M. Hara, *Langm.*, **29**, 4622 (2013).
14. R. Fernández, I. Mondragon, C. S. Rafaela, J. P. Felippe, N. O. J. Osvaldo, P. Oyanguren and M. J. Galante, *Mat. Sci. Eng. C.*, **33**, 1403 (2013).
15. M. L. Rahman, M. M. Yusoff, G. Hegde, M. N. F. A. Malek, N. A. Samah, H. T. Srinivasa and S. Kumar, *J. Chinese Chem. Soc.*, **61**(5), 571 (2014).
16. R. Dong, B. Zhu, Y. Zhou, D. Yan and X. Zhu, *Polym. Chem.*, **4**, 912 (2013).
17. W. D. Yun, J. Wang, D. W. Zhang and Z. T. Li, *Science China Chemistry*, **55**, 2018 (2012).
18. S. Balamurugan, G. Y. Yeap, W. A. K. Mahmood, P. L. Tan and K. Y. Cheong, *J. Photochem. Photobio. A: Chem.*, **278**, 19 (2014).
19. G. Binzet, U. Florke, N. Kulcu and Arslan, *Act. Cryst.*, **65**, 427 (2009).
20. A. D. Bautista, J. S. Appelbaum, C. J. Craig, J. Michel and A. Schepartz, *J. Am. Chem. Soc.*, **132**, 2904 (2010).
21. B. T. Gowda, S. Foro and H. Fuess, *Act. Cryst.*, **64**, 419 (2008).
22. B. T. Gowda, S. Foro, P. A. Suchetan, H. Fuess and H. Terao, *Act. Cryst.*, **E65**, 01998 (2009).
23. A. R. Yuvaraj, S. W. Gan, K. Ajaykumar, M. M. Yusoff and H. Gurumurthy, *RSC Adv.*, **4**, 50811 (2014).
24. G. N. M. Reddy, M. V. Kumar, T. N. G. Row and N. Suryaprakash, *Phys. Chem. Chem. Phys.*, **12**, 13232 (2010).
25. M. R. Lutfor, M. M. Yusoff, G. Hegde, M. N. Fazli, A. Malik and N. A. Samah, *Mol. Cryst. Liq. Cryst.*, **13**, 587, 41 (2013).
26. M. L. Rahman, S. Kumar, C. Tschierske, G. Israel, D. Ster and H Gurumurthy, *Liq. Cryst.*, **36**, 397 (2009).
27. M. L. Rahman, H. Gurumurthy, M. Azazpour, M. M. Yusoff and S. Kumar, *J. Fluor. Chem.*, **156**, 230 (2013).
28. G. Barbero, L. R. Evangelista and L. Komitov, *Phy. Rev. E.*, **65**, 041719 (2002).

Supporting Information

Photoisomerization behavior of photochromic amide based azobenzene dyes exhibiting H-bonding effect: Synthesis and characterization

Gurumurthy Hegde[*,†], Yuvaraj Aralapura Rajkumar[**], Gan Siew Mei[**], Syed Mahmood[***], Uttam Kumar Mandal[***], and Achalkumar Ammathnadu Sudhakar[****]

*BMS R and D Centre, BMS College of Engineering, Basavanagudi, Bangalore 560019, India
**Faculty of Industrial Sciences and Technology, University Malaysia Pahang, 26300, Gambang, Kuantan, Malaysia
***Department of Pharmaceutical, Technology, Kulliyyah of Pharmacy, International Islamic University, Malaysia (IIUM), Pahang Darul Makmur, Malaysia
****Department of Chemistry, Indian Institute of Technology, Guwahati, 781039, Guwahati - Assam, India
(*Received 1 July 2015 • accepted 26 November 2015*)

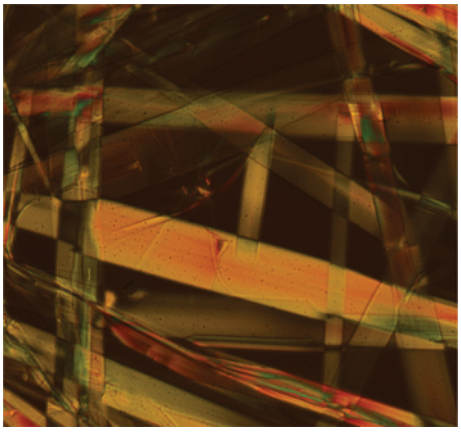

Fig. S1. Observed liquid crystalline behaviour for reported compounds. All four compounds showed similar kind of liquid crystalline texture where suddenly it changed from liquid crystal to crystalline.

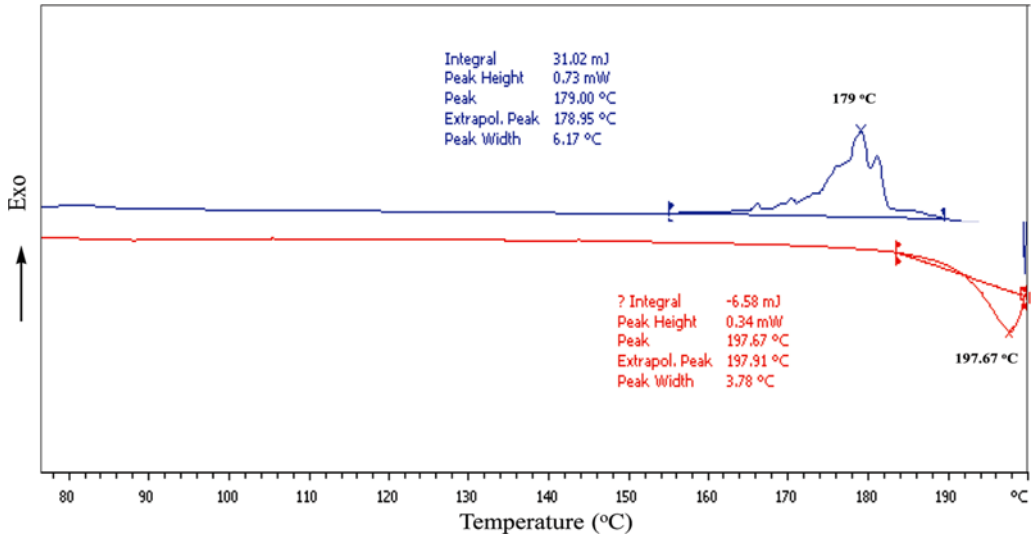

Fig. S2. DSC thermograms for the compound E_1.

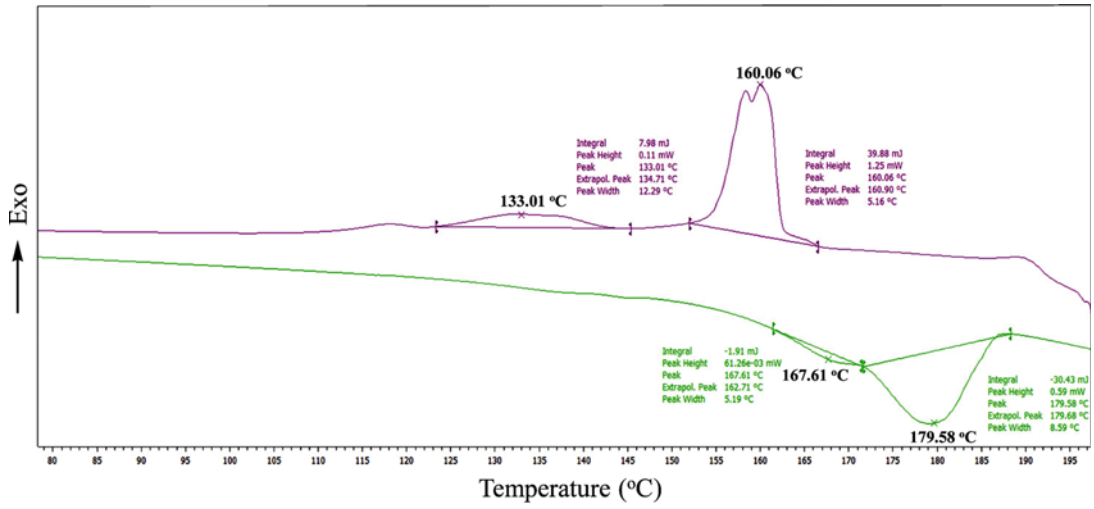

Fig. S3. DSC thermograms for the compound E_2.

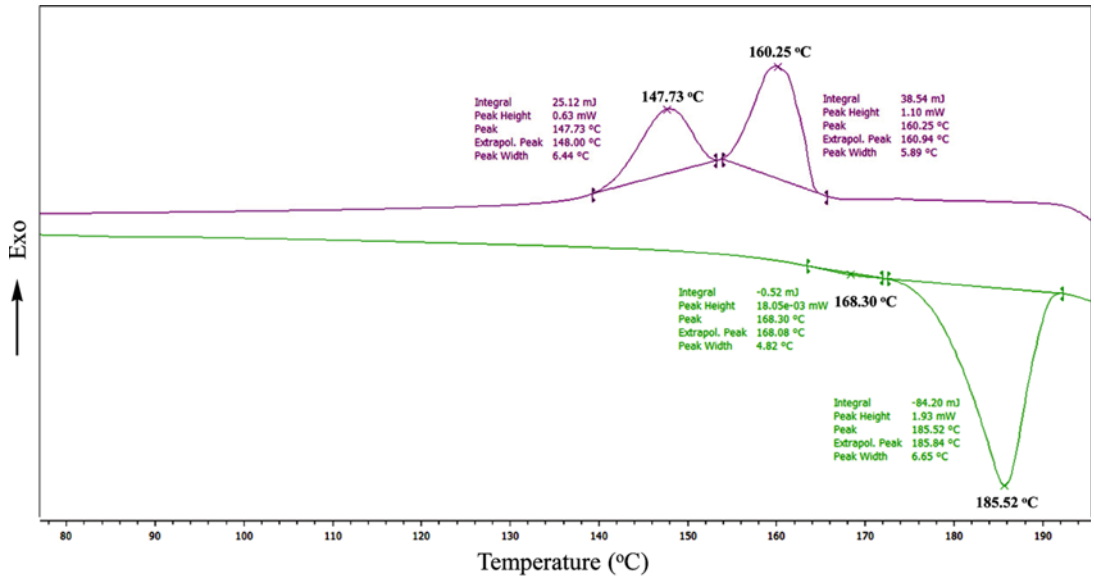

Fig. S4. DSC thermograms for the compound E_4.

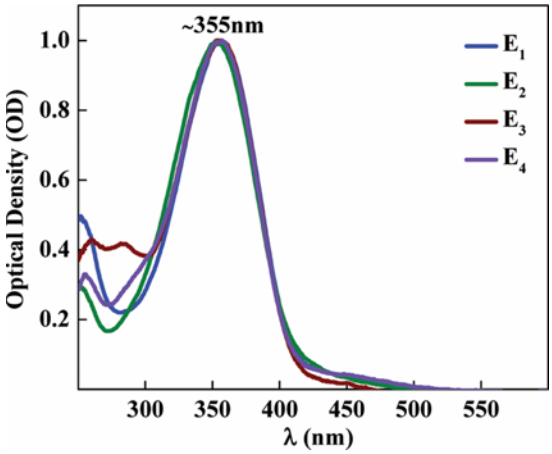

Fig. S5. The absorption spectra of E_1-E_4 show same peak absorption due to the similarity in their molecular structures.

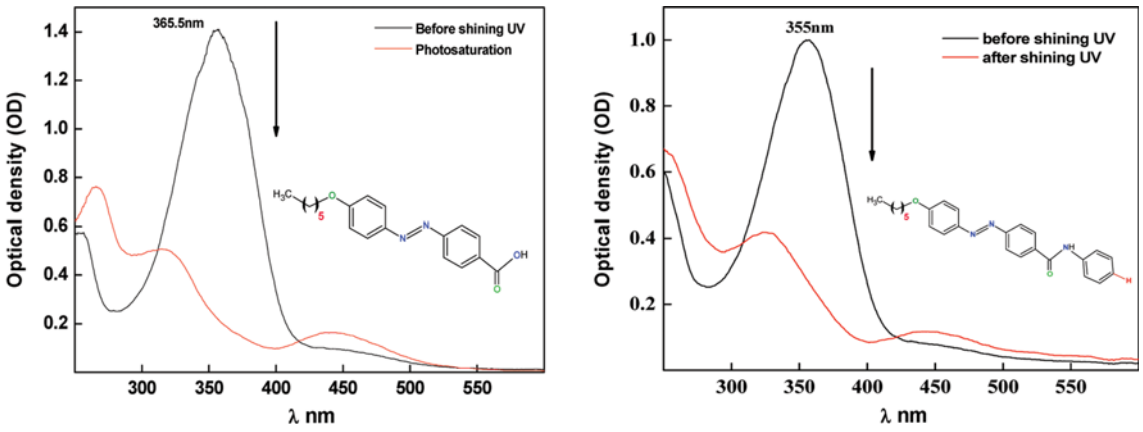

Fig. S6. The photo-saturation of the intermediate compound D (left) and E1 (right) was determined and measured the conversion efficiency. Further, the measurement has been done to justify the effect of hydrogen bonding in amide linkage.

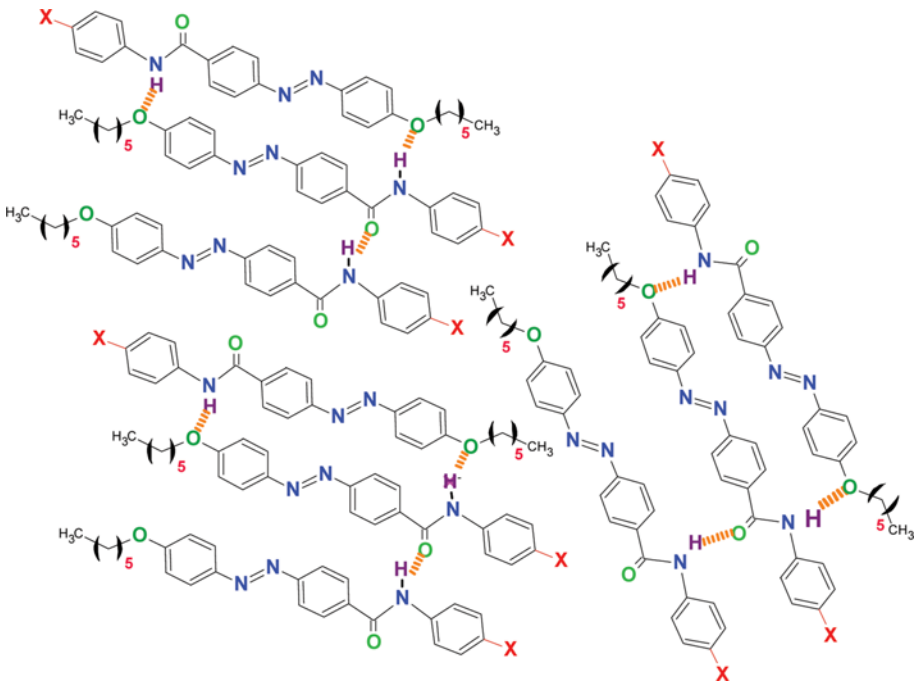

Fig. S7. The concept of intermolecular H-bonding in E_1-E_4.

Table S1. The Photoisomerization properties with different intensities for compound E_4

Intensity (in mW/cm^2)	Photosaturation (in sec)	Back relaxation (in hours)
2.380	29	10.93
5.860	24	10.58
9.020	19	8.95
13.200	16	7.84
17.590	10	6.38

Table S2. The extent of photoisomerization or conversion efficiency (CE) of amide based azodyes

Compounds	Extent of isomerization (%)
E_1	72
E_2	52
E_3	75
E_4	75

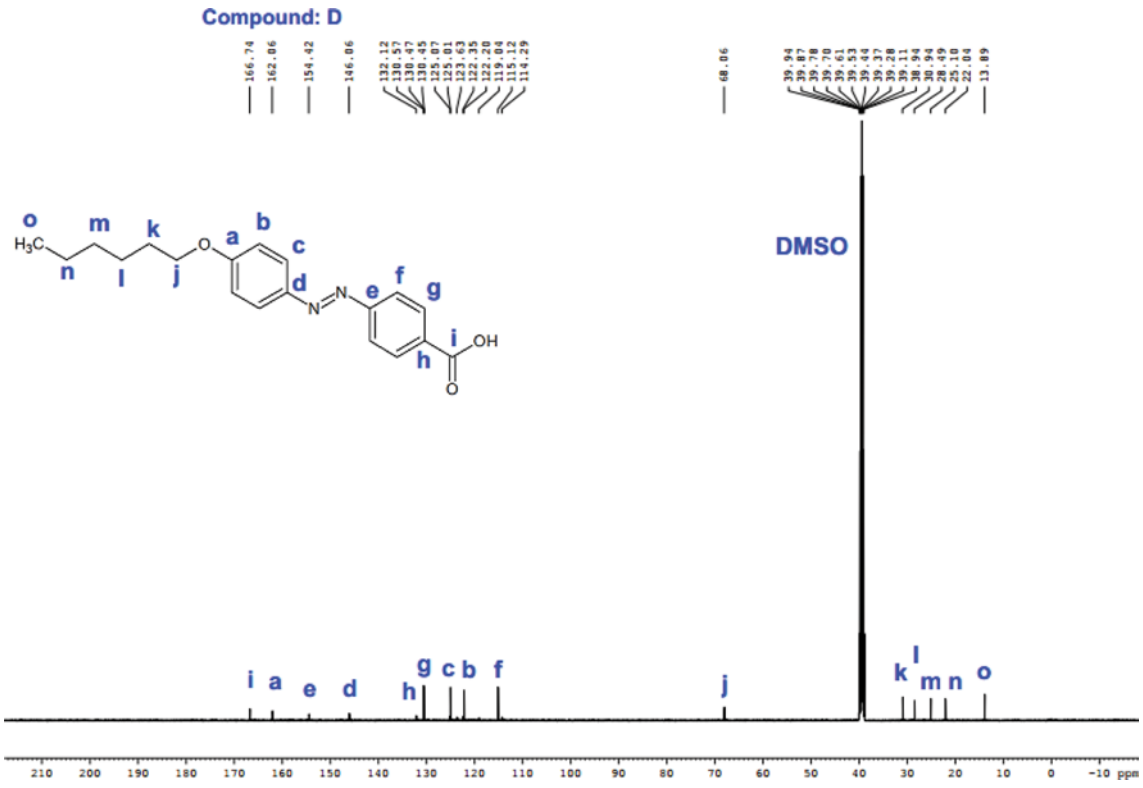

Fig. S8. ^{13}C NMR for compound D.